

# Measuring Supermassive Black Holes in Distant Galaxies with Central Lensed Images

David Rusin<sup>1</sup>, Charles R. Keeton<sup>2</sup>, Joshua N. Winn<sup>3,4</sup>

## ABSTRACT

The supermassive black hole at the center of a distant galaxy can be weighed, in rare but realistic cases, when the galaxy acts as a strong gravitational lens. The central image that should be produced by the lens is either destroyed or accompanied by a second central image, depending upon the mass of the black hole. We demonstrate that when a central image pair is detected, the mass of the black hole can be determined with an accuracy of  $\lesssim 0.1$  dex if the behavior of the smooth mass distribution near the galaxy core is known. Uncertainty in the central mass distribution introduces a systematic error in the black hole mass measurement. However, even with nearly complete ignorance of the inner mass distribution, the black hole mass can still be determined to within a factor of 10. Central image pairs should be readily observed with future radio interferometers, allowing this technique to be used for a census of supermassive black holes in inactive galaxies at significant redshift ( $0.2 \lesssim z \lesssim 1.0$ ).

*Subject headings:* galaxies: nuclei—black hole physics—gravitational lensing

## 1. Introduction

Supermassive black holes reside at the centers of most galaxies, and are therefore linked to a wide range of astrophysical phenomena. Most spectacularly, gas accretion onto a supermassive black hole (SMBH) is the power source for quasars and other active galaxies, and produces non-thermal emission spanning more than fifteen decades in wavelength. Among nearby galaxies, empirical correlations have recently been discovered between the mass of the SMBH and various galactic properties such as the bulge mass (Laor 2001), velocity dispersion (Ferrarese & Merritt 2000; Gebhardt et al. 2000; Tremaine et al. 2002), luminosity (Magorrian et al. 1998; McLure & Dunlop 2001, 2002), and concentration (Graham et al. 2001). The existence of these correlations is an intriguing cosmological clue, as it suggests that there has been an interplay between black hole

---

<sup>1</sup>Department of Physics & Astronomy, University of Pennsylvania, 209 So. 33rd St., Philadelphia, PA 19104-6396

<sup>2</sup>Department of Physics & Astronomy, Rutgers University, 136 Frelinghuysen Road, Piscataway, NJ 08854

<sup>3</sup>Harvard-Smithsonian Center for Astrophysics, 60 Garden St., Cambridge, MA 02138

<sup>4</sup>Hubble Fellow

growth and galaxy formation (e.g., Kauffmann & Haehnelt 2000; Monaco, Salucci & Danese 2000; Wyithe & Loeb 2002; Haiman, Ciotti & Ostriker 2004).

An important step forward would be to trace the evolution of these correlations over cosmic time (see, e.g., Treu, Malkan & Blandford 2004). For this, we need a way to measure central black hole masses in galaxies that are located at significant redshift. Two techniques have provided most of the existing black hole mass measurements. First, in normal galaxies, the SMBH mass can be determined from the kinematics of stars or gas near the galaxy center (Magorrian et al. 1998; Gebhardt et al. 2003). Although this method offers very accurate masses, it requires spectroscopy with high spatial resolution that can only be achieved for nearby galaxies. Second, in reverberation mapping of active galaxies (Blandford & McKee 1982; Kaspi et al. 2000; Peterson et al. 2004), the orbital parameters of gas clouds can be estimated from the width of the broad emission lines and the time lag between continuum and line variability, yielding a measurement of the SMBH mass. This method works at higher redshift, but it cannot be applied to normal, quiescent galaxies.

Gravitational lensing supplements these techniques by offering a way to detect and measure SMBHs in ordinary galaxies at intermediate redshift ( $0.2 \lesssim z \lesssim 1.0$ ). The starting point is the generic prediction that the multiple lensed images of a background object should include a faint image that appears close to the center of the lens (Burke 1981). A SMBH in the lens galaxy will alter the properties of this image, in one of two ways (Mao, Witt & Koopmans 2001). For certain SMBH masses and source positions, the black hole destroys the central image. If that does not happen, then the SMBH creates an *additional* image near the galaxy center. In other words, seeing a pair of central images is direct evidence for a supermassive black hole in the lens galaxy.

Radio observations seem to be the likeliest route to finding central images, because of the necessary angular resolution and dynamic range, and because dust extinction is not a problem at radio wavelengths. Bowman, Hewitt & Kiger (2004) recently calculated the probability of finding central image pairs produced by a SMBH, and concluded that the next generation of radio telescopes is needed to discover them in large numbers. In this Letter, we investigate what will be learned when a central image pair is detected: namely, with what accuracy can the mass of the SMBH be measured? The issue is timely because the best candidate for a central image has recently been found in the lens system PMN J1632–0033 (Winn, Rusin & Kochanek 2003b, 2004). Since the central image has apparently not been destroyed in that system, there must be a faint companion image if the lens galaxy hosts a SMBH.

Section 2 reviews the phenomenology of central images. Section 3 presents an analysis of simulated central image systems. In § 4 we discuss our results and outline several observational challenges. Standard values for the cosmological parameters ( $\Omega_m = 0.3$ ,  $\Omega_\Lambda = 0.7$ , and  $H_0 = 65 \text{ km s}^{-1} \text{ Mpc}^{-1}$ ) are assumed for all calculations.

## 2. The Phenomenology of Central Images

In the language of gravitational lensing theory (see, e.g., Kochanek, Schneider, & Wambsganss 2004), the formation of a central image requires the existence of at least one radial critical curve. In spherical models, this is equivalent to having at least one solution of the equation  $d\alpha(r)/dr = 1$ , where  $\alpha(r)$  is the deflection angle and  $r$  is the image-plane radius. Many commonly used mass models have exactly one such solution. Examples include the non-singular isothermal sphere (NIS), and single or broken power-law profiles with an inner slope that is shallower than isothermal ( $\rho \propto r^{-\beta}$  with  $\beta < 2$ ). Such models produce one central image, and have been described in detail by Wallington & Narayan (1993), Rusin & Ma (2001) and Keeton (2003).

A massive compact object at the center of the lens modifies the properties of central images because it dominates the deflection at small radii. We illustrate this phenomenon in Figure 1 using a NIS model. Intersections of the deflection profile  $\alpha(r)$  and the line  $r - u$  (where  $u$  is the source-plane radius) mark the locations of images. The NIS by itself produces three images of any source within the radial caustic. We denote these images as A (minimum), B (saddle point) and C (maximum).<sup>1</sup> Adding a central point mass causes the deflection angle to diverge as  $r \rightarrow 0$ , qualitatively altering the critical structure of the lens. In this example, it creates a second radial critical curve. Consequently, a sufficiently misaligned source ( $u_1$ ) produces a second central image: a saddle point, denoted as D. In contrast, no central images can form if the source is well-aligned with the galaxy core ( $u_2$ ). The SMBH therefore either destroys the central image, or introduces a second one (Mao et al. 2001).

For a given mass profile, detectable central image pairs only form over a narrow range of black hole masses. We illustrate this by considering a spherical power-law (PL,  $\rho \propto r^{-\beta}$ ) galaxy at  $z = 0.5$  with a SMBH, and a source at  $z = 1.5$ . The models are normalized to have an Einstein radius of  $0''.75$ , corresponding to a typical lens galaxy: a nearly  $L_*$  elliptical galaxy with velocity dispersion  $\sigma_* \approx 215 \text{ km s}^{-1}$ . Our definition of “detectable” is  $\mu_C/\mu_A > 10^{-2.5}$  and  $\mu_D/\mu_C > 10^{-2}$ , where  $\mu$  is the magnification. This is intended to simulate a realistic survey in which systems with detectable maximum-time images are sought first, and then followed up with more sensitive observations to detect the saddle-point image produced by the SMBH.

In Figure 2 we plot the fraction of systems (technically, the fraction of the area inside the radial caustic) meeting these criteria as a function of  $M_{BH}$ .<sup>2</sup> For each galaxy profile ( $1.75 \leq \beta \leq 1.95$ ), detectable central images form over a black hole mass range spanning less than one decade. The high-mass cutoff occurs where the SMBH destroys the central images, a threshold that is independent of the detectability criteria. The low-mass cutoff is enforced by the lower bound on

---

<sup>1</sup>The terminology indicates whether the image forms at a minimum, saddle point, or maximum in the time delay surface (Schneider 1985, Blandford & Narayan 1986).

<sup>2</sup>The results can be generalized to any Einstein radius, black hole mass, cosmology and redshifts by noting that they depend only on the ratio  $M_{BH}/M_{Ein}$ , where  $M_{Ein}$  is the projected mass of the PL within  $R_{Ein}$ .

$\mu_C/\mu_A$ . Thus, smaller black holes could be detected with more sensitive observations. In contrast, relaxing the requirement on  $\mu_D/\mu_C$  increases the fraction of detectable systems for a given black hole mass, but does not extend the detectable black hole mass range.

The mass range that produces central image pairs is (fortuitously) coincident with astrophysically realistic SMBHs. By using an isothermal approximation to relate the image separation to the velocity dispersion, we use the local  $M_{BH}-\sigma$  relation (Tremaine et al. 2002) to predict that the SMBH should have a mass of  $\log(M_{BH}/M_\odot) = 8.2 \pm 0.2$  in our example galaxy—well within the favored range for most mass profiles (Fig. 2). Consequently, gravitational lensing offers a means of detecting and measuring SMBHs in intermediate-redshift galaxies.

### 3. Monte Carlo Simulations

Our goal is to investigate how accurately the mass of the SMBH can be recovered from realistic observations of a central image pair. It is especially important to study the systematic errors associated with the uncertainty in the smooth mass distribution of the lens galaxy. Because a pair of central images has not yet been detected in any real gravitational lens system, we must investigate constraints on supermassive black holes using simulated lenses.

We create simulated lenses using a PL model with a central point mass, and an external shear field of 10% to mimic the effects of galaxy ellipticity and nearby perturbers. For simplicity the Einstein radius of the PL galaxy is fixed at the typical value of  $0''.75$ . We consider sub-isothermal logarithmic slopes of  $1.75 \leq \beta \leq 1.95$ , which are broadly consistent with many observed lens galaxies (see, e.g., Rusin, Kochanek & Keeton 2003; Winn et al. 2003b; Treu & Koopmans 2004). For each profile we investigate the values of  $M_{BH}$  which produce detectable central image pairs. We randomly place sources behind the deflector and solve for the image positions and magnifications. We focus exclusively on “doubles” (which have two bright images, but can have a total of four images, if central images are included) because they are the preferred systems for central image hunting. In “quads”, the central maximum is typically much fainter and far more susceptible to being extinguished by the SMBH. Furthermore, we limit ourselves to simulated “doubles” that meet the magnification ratio criteria described in § 2. Altering these criteria does not significantly affect any of the results presented below. We perturb the image data with typical errors for radio observations (positional uncertainties of 1 mas and flux errors of 20% on each image to account for possible substructure effects). We also perturb the galaxy position by 20 mas, a conservative estimate for the uncertainty in the lens galaxy centroid.

We fit the simulated lenses using models consisting of a spherically-symmetric mass profile to describe the galaxy (with one parameter modulating its concentration), a point mass coincident with the galaxy center, and an external shear field. The models have four degrees of freedom. We simultaneously optimize all model parameters using a standard  $\chi^2$  statistic, which includes contributions from the image positions and magnifications, as well as the galaxy position. We then

extract the distribution of best-fit values of  $\log M_{BH}$  for the ensemble of simulated lenses created from a given set of input parameters, and describe this distribution by its mean and standard deviation. For each individual lens we also calculate the range of acceptable  $\log M_{BH}$  using the  $\Delta\chi^2$  method, verifying that these uncertainties correspond closely to the standard deviation of the ensemble.

First we fit the data with a PL profile. We find that the input black hole mass can be recovered with an excellent accuracy of 0.05 – 0.10 dex in  $M_{BH}$ . The low scatter in the best-fit  $M_{BH}$  is undoubtedly related to the very tight simultaneous constraint we derive on the logarithmic density slope  $\beta$ . As modeling of the three-image lens PMN J1632–0033 has shown, even one central image (C) provides a tight constraint on the exponent of a PL mass profile (Winn et al. 2003b). The properties of image D then determine  $M_{BH}$ .

To investigate the systematic error that results from uncertainty in the galaxy mass model, we fit the simulated lens data with a NIS profile instead of a PL profile. These two profiles are qualitatively very different in the inner region where central images form, yet the lensing data alone may not be able to discriminate between them (see, e.g., Winn et al. 2003b). We find that a pair of central images does no better than a single central image in distinguishing between PL and NIS galaxies. Furthermore, fitting with a NIS model yields black hole masses that are systematically larger than the “true” (PL) values. Figure 3 shows the systematic offset at a single input  $M_{BH}$  for different input  $\beta$ . The offset is 0.6 dex for  $\beta = 1.75$ , and gradually rises to 1.0 dex at  $\beta = 1.95$ . For the PL slope that best fits PMN J1632–0033 ( $\beta = 1.90$ ), the offset is 0.8 dex. (At fixed input  $\beta$ , the offset is a very weak function of the input  $M_{BH}$ , varying by less than 0.1 dex over the entire range of black hole mass producing detectable central image pairs.)

These results show that uncertainty in the inner mass profile of the galaxy will systematically affect the inferred mass of the SMBH. Fortunately, there is a finite range of inner slopes that are expected for a realistic galaxy, and the PL and NIS models bracket this range. First, because the density is expected to decrease monotonically with radius, the shallowest possible profile is a finite-density core. Second, galaxy mass profiles are always observed to become shallower at smaller radius, rather than steeper (Byun et al. 1996; Ravindranath et al. 2001). Hence the inner profile is not steeper than the best-fit global power-law profile. We conclude that the PL versus NIS analysis yields a nearly maximal systematic error estimate for the black hole mass.

To further investigate systematic errors related to the central mass distribution of the galaxy, we introduce a broken power-law (BPL) model for which the surface density varies as  $r^{-\gamma_{in}}$  for  $r < r_0$ , and  $r^{-\gamma_{out}}$  for  $r \geq r_0$ . By fixing the outer slope at the isothermal value ( $\gamma_{out} = 1$ ), the BPL can represent both the NIS (for  $\gamma_{in} = 0$ ) and the PL (for  $r_0 \rightarrow \infty$ ). In Figure 4 we show the results of fitting the BPL model to the simulated data that were generated with a PL model.<sup>3</sup>

---

<sup>3</sup>Results are shown for the particular input parameters  $\beta = 1.80$  and  $\log(M_{BH}/M_{\odot}) = 8.0$ , which are representative of those derived for other choices of input parameters.

There are three findings of the BPL analysis. First, as before, we find that it is not possible to use the data to distinguish between different values of  $\gamma_{in}$ . Second, we find that the recovered  $\log M_{BH}$  varies systematically with the inner slope. For  $\gamma_{in} = 0$ , the mean value is slightly higher than our estimate using the NIS. For  $\gamma_{out} = 0.8$  ( $\beta = 1.80$ ) we recover the input PL value very accurately. Finally, we find that the inferred  $\log M_{BH}$  is a stronger function of  $\gamma_{in}$  when that slope is shallow, as opposed to steep (Fig. 4). Most of the variation in  $\log M_{BH}$  occurs just as the model is reaching the PL limit. Thus, even a crude determination of whether  $\gamma_{in}$  is shallow or steep (from other observations) could substantially reduce the systematic error. Empirically, Byun et al. (1996) and Ravindranath et al. (2001) find that the majority of local elliptical galaxies have inner surface brightness slopes (and, hence, inner surface density slopes) that are shallower than  $\gamma_{in} = 0.6$ .

Besides an estimate of the inner density slope, can any combination of improved constraints help to discriminate between the PL and NIS models, and thus reduce the systematic error? We investigated three initially promising ideas: (1) a very precisely determined galaxy center ( $\sim 1$  mas), which could be obtained by detecting emission from a low-level active nucleus associated with the SMBH; (2) well-measured time delays ( $\sim 0.5$  day) among all images; and (3) the requirement that the mass quadrupole be aligned with the observed position angle of the lens galaxy to within  $20^\circ$  (see, e.g., Kochanek 2002; Winn, Hall, & Schechter 2003a). Unfortunately, our simulations show that these constraints, even in combination, do not completely break the degeneracy between the inner density profile and the inferred black hole mass. For example, the time delays among B, C and D are typically too short to be useful, and the shear constraint adds little information because the models already closely recover the input shear direction. Most promising is the constraint on the black hole position, which in some cases can distinguish between the PL and NIS models at the  $2\text{--}3\sigma$  level. Of course, it is not necessarily true that the AGN precisely marks the center of the galaxy mass distribution.

#### 4. Discussion

A pair of central images is the expected signature of a supermassive black hole in the core of a lens galaxy. Previous studies have described the phenomenology of these images (Mao et al. 2001), and the likelihood of detecting such systems in future radio surveys (Bowman et al. 2004). In this Letter we have considered the utility of a central image pair in measuring the mass of the SMBH. This issue is timely because the best candidate for a central image has recently been discovered (Winn et al. 2003b, 2004), and a search is underway to find the companion image that must be present if the lens galaxy hosts a supermassive black hole.

We investigated the possibility for SMBH measurements by creating and modeling simulated lens systems. There are two main results. First, if we know the inner mass distribution of the galaxy—specifically, its density slope over the region where central images appear—then realistic observations of the central image pair allow  $M_{BH}$  to be determined to within 0.1 dex. Second, uncertainty in the inner mass distribution introduces a significant systematic error in  $M_{BH}$ . Our

simulated lens data were fitted equally well with a power-law (PL) and a non-singular isothermal sphere (NIS), but the inferred values of  $M_{BH}$  were 0.6–1.0 dex larger for the NIS fit. On physical and empirical grounds, we believe that this is the maximum systematic error in  $M_{BH}$  determinations. We also used a broken power-law (BPL) model to explicitly demonstrate the dependence of  $M_{BH}$  on the inner profile slope.

Although the systematic error weakens our ability to measure SMBH masses, we believe that the lensing technique described above will prove of great utility. We are not aware of any other proposed method for the direct measurement of black hole masses in distant, inactive galaxies. Furthermore, we note that the maximum systematic error for SMBHs at *intermediate redshift* is only about 2–3 times larger than the statistical error on mass measurements for *local* black holes. The systematic error could be eliminated by directly measuring the central luminosity (and hence mass) profile of the lens galaxy, though this will be extremely difficult even with the next generation of space-based telescopes. An alternative would be to apply priors based on observations of local ellipticals (e.g., Byun et al. 1996; Ravindranath et al. 2001).

Apart from the high sensitivity that is needed to detect central image pairs in large numbers (Bowman et al. 2004), there are some additional observational challenges. Free-free absorption by ionized material close to the lens galaxy center could cause problems in detecting central images (see Winn et al. 2003b). Observations at high frequencies may be required to ensure that flux ratios are not affected by absorption. Microlensing could also complicate the determination of image magnifications. One would need to rely on the usual lens tests—a common spectrum, surface brightness, and correlated variability—to show that a radio source is actually a central image rather than a low-level AGN in the core of the lens galaxy.

Future observations with the Square Kilometer Array offer the best hope for successfully overcoming these issues and discovering large samples of lenses with central image pairs. Since the outer images reveal the galaxy mass, and the central image pairs determine the black hole mass, this instrument may allow us to investigate the evolution of the black hole–galaxy connection.

The authors wish to thank Avi Loeb and Chris Kochanek for helpful discussions.

## REFERENCES

- Blandford, R., & McKee, C.F. 1982, *ApJ*, 255, 419
- Blandford, R., & Narayan, R. 1986, *ApJ*, 310, 568
- Bowman, J.D., Hewitt, J.N., & Kiger, J.R. 2004, *ApJ*, in press (astro-ph/0406568)
- Burke, W.L. 1981, *ApJL*, 244, L1
- Byun, Y.-I., Grillmair, C.J., Faber, S.M., Ajhar, E.A., Dressler, A., Kormendy, J., Lauer, T.R., Richstone, D., & Tremaine, S. 1996, *AJ*, 111, 1889
- Ferrarese, L., & Merritt, D. 2000, *ApJL*, 539, L9
- Gebhardt, K., et al. 2000, *ApJL*, 539, L13
- Gebhardt, K., et al. 2003, *ApJ*, 583, 92
- Graham, A.W., Erwin, P., Caon, N., & Trujillo, I. 2001, *ApJ*, 563, L11
- Haiman, Z., Ciotti, L., & Ostriker, J.P. 2004, *ApJ*, 606, 763
- Kaspi, S., Smith, P.S., Netzer, H., Maoz, D., Jannuzi, B.T., Giveon, U. 2000, *ApJ*, 533, 631
- Kauffmann, G., & Haehnelt, M. 2000, *MNRAS*, 311, 576
- Keeton, C.R. 2003, *ApJ*, 582, 17
- Kochanek, C.S. 2002, in *Proceedings of the Yale Cosmology Workshop: The Shapes of Galaxies and Their Dark Matter Halos*, P. Natarajan, ed. (Singapore: World Scientific)
- Kochanek, C.S., Schneider, P., & Wambsganss, J. 2004, Part 2 of *Gravitational Lensing: Strong, Weak & Micro*, *Proceedings of the 33rd Saas-Fee Advanced Course*, G. Meylan, P. Jetzer & P. North, eds. (Berlin: Springer-Verlag) (astro-ph/0407232)
- Laor, A. 2001, *ApJ*, 553, 677
- Magorrian, J., et al. 1998, *AJ*, 115, 2285
- Mao, S., Witt, H.J., & Koopmans, L.V.E. 2001, *MNRAS*, 323, 301
- McLure, R.J., & Dunlop, J.S. 2001, *MNRAS*, 327, 199
- McLure, R.J., & Dunlop, J.S. 2002, *MNRAS*, 331, 795
- Monaco, P., Salucci, P., & Danese, L. 2000, *MNRAS*, 311, 279
- Peterson, B.M., et al. 2004, *ApJ*, 613, 682
- Ravindranath, S., Ho, L.C., Peng, C.Y., Filippenko, A.V., & Sargent, W.L.W. 2001, *AJ*, 122, 653
- Rusin, D., & Ma, C.-P. 2001, *ApJL*, 549, L33
- Rusin, D., Kochanek, C.S., & Keeton, C.R. 2003, *ApJ*, 595, 29
- Schneider, P. 1985, *A&A*, 143, 413
- Tremaine, S., et al. 2002, *ApJ*, 574, 740



- Treu, T., & Koopmans, L.V.E. 2004, *ApJ*, 611, 739
- Treu, T., Malkan, M.A., & Blandford, R.D. 2004, *ApJL*, 615, L97
- Wallington, S., & Narayan, R. 1993, *ApJ*, 403, 517
- Winn, J.N., Hall, P., & Schechter, P.L. 2003a, *ApJ*, 597, 672
- Winn, J.N., Rusin, D., & Kochanek, C.S. 2003b, *ApJ*, 587, 80
- Winn, J.N., Rusin, D., & Kochanek, C.S. 2004, *Nature*, 427, 613
- Wyithe, J.S.B., & Loeb, A. 2002, *ApJ*, 581, 886

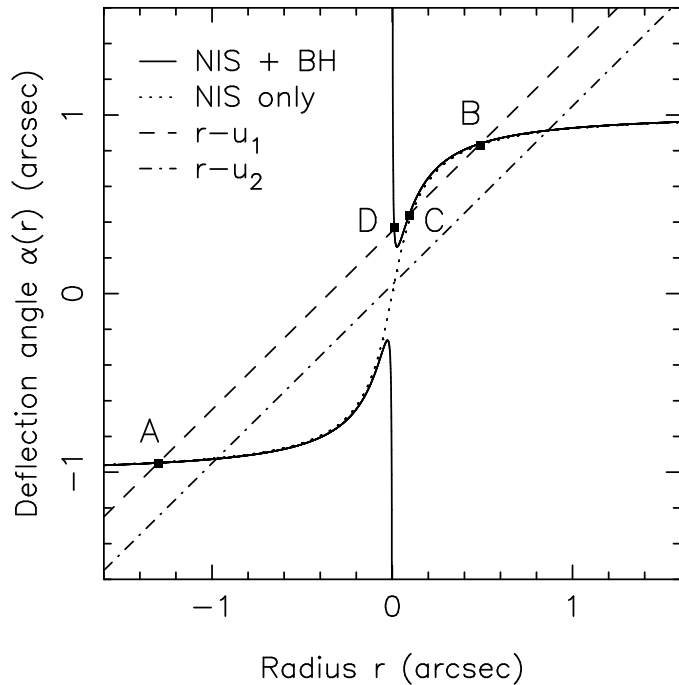


Fig. 1.— The phenomenology of central images, as illustrated by a NIS model. We plot the deflection profile  $\alpha(r)$  with (solid line) and without (dotted line) a central black hole. Intersections of  $\alpha(r)$  and the line  $r - u$  (where  $u$  is the source position) mark the locations of lensed images. The NIS alone produces three images (A, B, C) of any source within the radial caustic. In the presence of a central black hole, a fourth image (D) is produced for sufficiently misaligned sources ( $u_1$ , dashed line), while for well-aligned sources image C is destroyed ( $u_2$ , dashed-dotted line).

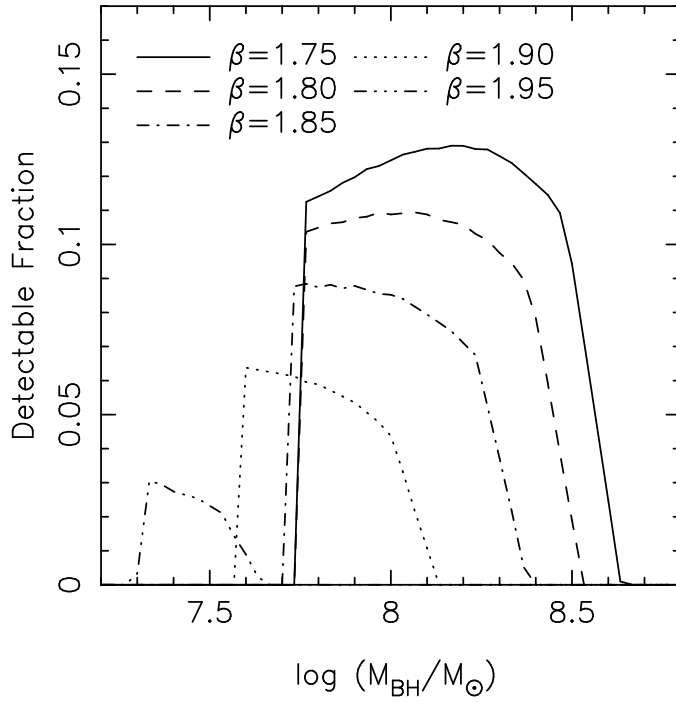


Fig. 2.— The detectability of central image pairs produced by a PL galaxy with a supermassive black hole. We plot the fraction of source positions inside the radial caustic that satisfy image magnification ratio cuts of  $\mu_C/\mu_A > 10^{-2.5}$  and  $\mu_D/\mu_C > 10^{-2}$ . The lens redshift is 0.5, the source redshift is 1.5, and the Einstein radius is  $0''.75$  for these and all subsequent simulations. We show results for five different profile slopes, spanning the range  $1.75 \leq \beta \leq 1.95$ . According to the local  $M_{BH}-\sigma$  relation, the model galaxy should have a SMBH with  $\log(M_{BH}/M_{\odot}) = 8.2 \pm 0.2$ .

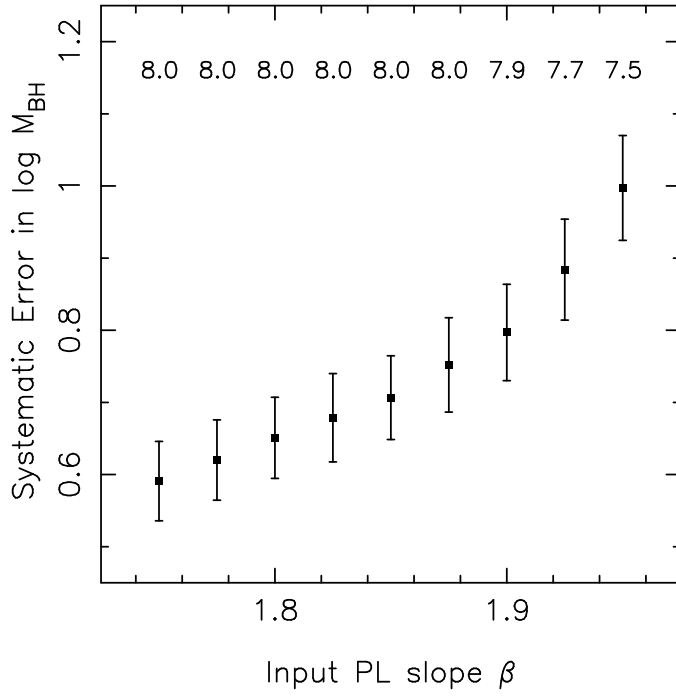


Fig. 3.— Systematic errors in black hole mass measurement. For each input PL slope  $\beta$ , we consider a representative black hole mass (note the values of  $\log(M_{BH}/M_{\odot})$  listed above the data points) that produces detectable central images. Simulated lenses are created with a PL model and fitted with a NIS model. We plot the difference between the mean recovered value of  $\log M_{BH}$  using the NIS model, and the input  $\log M_{BH}$ . Values of  $M_{BH}$  extracted using the NIS are systematically larger than the PL values by 0.6–1.0 dex. Note that for a given  $\beta$ , the systematic offset decreases mildly with increasing input  $M_{BH}$ , varying by less than 0.1 dex over the range of  $M_{BH}$  producing detectable central image pairs.

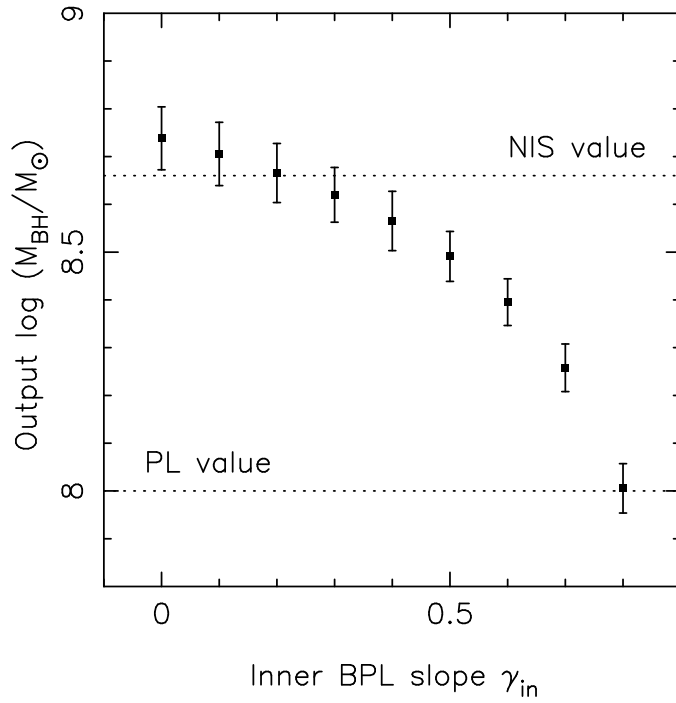


Fig. 4.— Systematic errors related to the inner profile slope. Simulated lens systems, created from a PL mass distribution with slope  $\beta = 1.80$  and  $\log(M_{BH}/M_{\odot}) = 8.0$ , are fitted with a BPL surface density model with outer slope  $\gamma_{out} = 1$ . We plot the mean value of  $\log M_{BH}$  extracted from the BPL fit, and find that it varies systematically with the inner BPL slope  $\gamma_{in}$ . Also shown are the input  $\log M_{BH}$  and the mean value extracted from a fit using a NIS, which can be approximated by a BPL with  $\gamma_{in} = 0$ .